Zheng LI, Zhihu GUO

School of Electrical Engineering, Hebei University of Science and Technology

Modelling and Spherical Air Bearing Based Levitation Design of a Novel M-DOF Actuator

Abstract. *Supporting and levitation control are important for actuators or motors with complicated structures. Based on the presented configuration design, the simplified torque calculation model and non-linear system dynamic model have been proposed, and spherical air bearing levitation mechanism is developed for alleviating the friction and resistance to improve the dynamic performance of this m-DOF actuator. The fluid field model is built in computational fluid dynamics software. Different structure parameters and conditions are computed and compared with the pressure distribution characteristics. Experiment results show that the actuator can effectively implement 3-DOF motion with the designed levitation modes, and that the proposed approach can be applied to m-DOF actuators of the same kind effectively.*

Streszczenie. *W artykule przedstawiono wyniki prac nad mechanizmem lewitacji w powietrznym łożysku kulistym siłownika typu m-DOF, mających na celu zwiększenie dynamiki poprzez zmniejszenie tarcia i rezystancji. Zaproponowano także uproszczoną metodę obliczania momentu mechanicznego oraz model układu w stanach dynamicznych. Opracowane modele lewitacji zostały poddane weryfikacji eksperymentalnej. (**Modelowanie siłownika typu M-DOF – lewitacja w powietrznym łożysku kulistym**)*

Keywords: Air bearing, levitation, m-DOF, actuator.
Słowa kluczowe: Łożysko powietrzne, lewitacja, m-DOF, siłownik.

Introduction

With the development of the industry and technology, robot and manipulators which can achieve three-degree-of-freedom (3-DOF) motion are used more and more widely. This kind of devices are usually built with several convention driver motor, each having single degree-of-freedom, which reduces the position accuracy, efficient, dynamic performance of the system. In this condition, the m-DOF actuators or motors have attracted many attentions [1-5]. To realize precision control, the feedback control system is necessary. However, the support mechanism design with measurement systems used for single-DOF feedback control system is not suitable for the m-DOF feedback control system. So the bearing design and control becomes a crucial problem and should be paid more attentions. There are mainly four methodologies to support the m-DOF spherical rotor recently. These methods are classified into two kinds of contact and noncontact methods. Because of the flaws of contact measurement method, using the non-contract method is the development trends of the bearing design. In the design of PM spherical actuator structure, the supporting structure is very important. According to the original content, design and analysis of the actuator structure, due to the actuator's unique three-dimensional spherical structure, making the use of contact ball bearing, the implementation is not entirely suitable for full rotation speed range and non-contact feature can be applied to complex three-dimensional structure of the bearing and lubrication. This paper mainly presents the modeling and application of the spherical air bearing levitation mechanism for supporting the m-DOF rotor with satisfied performance.

Operation principle and dynamic analysis of m-DOF PM actuator

The motor prototype consists of a ball-shaped rotor with four layers of 40 poles and two layers of 24 poles. There are 10 poles with equally spaced position of alternative N-S distribution for the rotor. There are 12 poles in each layer and controlled separately for the stator. Figure 1 shows the basic structure of the actuator. The actuator is designed to implement maximum 67 degrees tilt motion and 360 degrees rotation.

Using the Lagrange energy method, the dynamic equations of multi-DOF actuator are obtained. Each equation represents an axis of Cardian Angle. It can be seen that there are many one-order and two-order coupling terms in the equation, which indicates serious inter-axes nonlinear coupling of the spherical actuator.

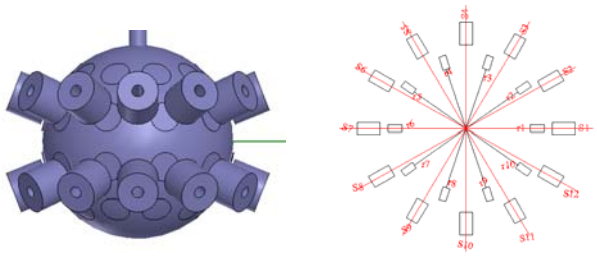

Fig.1. Basic structure of the actuator

Like the conventional reluctance motors, the operation of the actuator is also based on the reluctance forces. The difference is that the flux path is not closed due to the non-magnetic material used in the rotor. It can be considered that the torque or force exerted on the rotor is the summation of individual rotor/stator pair interactions and the torque calculation model has the linear property.

The torque equation can be combined into one vector equation in the x-y-z coordinate [6-8]:

$$\mathbf{T} = \frac{1}{2}\sum_{j=1}^{n_r}\sum_{k=1}^{n_s}\frac{\partial \Lambda_{jk}}{\partial \delta_{jk}} F_{jk}^2 \frac{\mathbf{r}_{rj}\times\mathbf{r}_{sk}}{\left\|\mathbf{r}_{rj}\times\mathbf{r}_{sk}\right\|} \tag{1}$$

From equation (1), the torque calculation has been simplified to the superposition of torque component by individual pair as shown in figure 2. The former two parameters can be taken as torque constant, and derived by accurate computation or experiments. The torque produced by single stator/rotor pair can be written as

$$\mathbf{T_{jk}} = k(\delta_{jk}, i_k)\frac{\mathbf{r}_{rj}\times\mathbf{r}_{sk}}{\left\|\mathbf{r}_{rj}\times\mathbf{r}_{sk}\right\|} Ni_j \tag{2}$$

where the constant $k(\delta_{jk}, i_k) = \dfrac{\left\|\mathbf{T_{jk}}\right\|}{Ni_j}$ is a function of δ_{jk} and i_k, so in the case of the reference torque is known, the control current corresponding to some rotor orientation can be solved by

(3) $$\mathbf{T} = \mathbf{K_T I_d}$$

(4) $$\mathbf{I_d} = \mathbf{K_T}^{+}\mathbf{T}$$

where $\mathbf{K_T}$ is the torque constant matrix about some orientation, $\mathbf{K_T}^{+}$ denotes its general inverse matrix. $\mathbf{I_d}$ is the reference control current.

By development and substitution, the complete mathematical model of the system can be written as

(5) $$\mathbf{M(Q)}\ddot{\mathbf{Q}} + \mathbf{C(Q,\dot{Q})}\dot{\mathbf{Q}} + \mathbf{G(Q)} + \mathbf{T_{Qf}} = \mathbf{T_{Qe}}$$

where

$$\mathbf{M(Q)} = \mathbf{J_Q^T M_r J_Q} = \begin{pmatrix} J_{ba}c\beta^2 + J_b s\beta^2 & 0 & J_b s\beta \\ 0 & J_{ba} & 0 \\ J_b s\beta & 0 & J_b \end{pmatrix},$$

$$\mathbf{C(Q,\dot{Q})} = \mathbf{J_Q^T M_r}\,\dot{\mathbf{J}}_\mathbf{Q} + \mathbf{J_Q^T C_r J_Q},$$

$$\mathbf{G(Q)} = \mathbf{J_Q^T T_g} = m_c g r_c \begin{pmatrix} -s\alpha c\beta^2 c\gamma + s\beta c\beta s\gamma \\ -s\alpha c\beta s\gamma - s\beta c\gamma \\ 0 \end{pmatrix},$$

$$\mathbf{T_{Qf}} = \mathbf{J_Q^T T_f}, \qquad \mathbf{T_{Qe}} = \mathbf{J_Q^T T_e}$$

The nonlinear friction has a great effect on the servo system and is hard to derive accurate mathematical models. Here, the design is performed by confirming its upper bound ρ_f, and was estimated by

(6) $$\mathbf{T_{Qf}}(\dot{\mathbf{Q}}) = sign(\dot{\mathbf{Q}})\mathbf{T_c} + sign(\dot{\mathbf{Q}})(\mathbf{T_s} - \mathbf{T_c})\exp(-\mu|\ \dot{\mathbf{Q}}\ |)$$

where $\mathbf{T_s}$, $\mathbf{T_c}$, μ denote the static friction, coulomb friction and exponential constant.

The motor dynamics have the same form and properties as those of a robotic manipulator. The control scheme can be applied on the continuous trajectory tracking control, to minimize the effects of uncertainties including parameters perturbation, model error and outer disturbance.

Spherical air bearing based levitation schemes

In real applications, the air bearing and magnetic levitation principles are appropriate for the actuators with 3D structures. The air bear needs additional air source with large volume and relatively low control precision. The magnetic levitation usually performed with the decoupling of the electromagnetic system into torque and levitation sub-systems. However, the magnetic levitation is difficult to implement with large tilt angle of the rotor. So the most proper way for allevating the levitation problems is to using the spherical air bearing as the basic levitation mode especially for pan-tilt motions and also for uniform spin rotation motion.

In the design of permanent magnet multi-DOF actuator structure, the supporting structure is very important. According to the original content, design and analysis of the actuator structure, with due to the actuator's unique three-dimensional spherical structure, making use of hydraulic bearing is not entirely suitable for that the air bearing has a high flexibility and non-contact feature apply to complex three-dimensional structure of the bearing and lubrication. This paper focuses on the first application of air bearings in the motor with multiple degrees of freedom by exploration and study.

The structure of the air bearing can be shown in figure 2. There is a gas film among the rotor spherical surface and the stator ball socket. When the air with pressure Ps flows through the orifice into the air film, the pressure after the hole dropped to Pd, the sphere is moving along the axis of symmetry, each orifice pressure is bound to each other with equal value. The air outflows from the orifice to the outer boundary of the θ2 cone to flow directly into the atmosphere. The air pressure behind the orifice of Pd is gradually reduced to the boundary at ambient pressure Pa. Pd gradually become pressure Pa caused by the carrying capacity of the spherical bearing. Gas pressure in the horizontal projection of the sphere is symmetrical, so the horizontal force is zero, while in the vertical projection of oz axis to form a spherical bearing. When the floating amount h increases, the formation of the gas film thickness increases, so that the air flow resistance is smaller and the air flow increased, causing the pressure drop through the orifice increases. Pd will be reduced in the case of the outer supply pressure Ps keeps to the same, resulting in the total supporting force projection will also be smaller in the direction of oz axis. On the contrary, the combined force projection in the oz-axis direction will increase when the floating amount decreases. When the ball bearing structure and the gas pressure is constant, the floating amount is uniquely related to the carrying capacity.

For this study on the air flow of the ball bearings, the following assumptions can be adopted:

(1) The lubrication gas is taken as a Newtonian fluid; gas viscosity coefficient μ is constant;

(2) Gas membrane gas flow for the isothermal process, the boundary layer is fully developed laminar flow is stable;

(3) Do not consider the impact of gravity on the gas;

(4) Take the gas as an ideal gas.

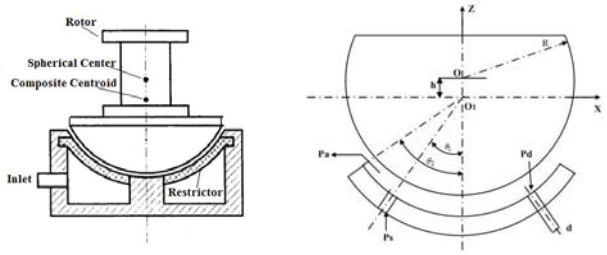

Fig.2. Illustration of the static pressure spherical air bearing

According to the assumptions, the control equation can be simplified to model calculations, based on the use of CFD software (the Fluent). This work uses CFD analysis software for the numerical calculation, so it is necessary to use pre-processing software for flow field modeling of the spherical bearings, and the mesh generation, mesh type, density, quality, and local processing will show a great effect on the computational efficiency and accuracy. As for the flow field numerical calculation, the gas film thickness is very thin (micron) and the thickness and circumference sizes are with difference of thousands of times. To reduce the computational truncation errors and preventing the calculation divergence, the hexahedral and pyramid grid are mainly used for meshing. Around the orifices with intense changes of expected pressure and speed, the structured hexahedral grids and local refinement are adopted. The volume mesh with air feed orifices is shown in figure 3.

CFD analysis software can be used for 2D and 3D model calculation, and also provides single-precision and double precision solvers. In most cases, the single-precision solver is efficient and accurate, but for the slender pipe model and the gas lubrication model, the direction of length scales show much difference, when describing the

coordinates of the nodes the single-precision grid computing would be not appropriate. Therefore, the 3D model of the double-precision solver is chosen.

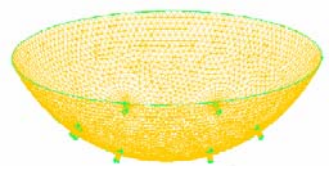

Fig.3. Mesh of the volume with the air feed holes

CFD analysis software also provides separation and coupling two solvers; two solutions are applicable to a wide range of pressure from incompressible to high-speed flow. When computing high-speed compressible flow, the coupled solver is with advantage of faster convergence. The memory needed with coupled solver is about 1.5 to 2 times that of the separation solver. In view of the gas lubrication problem, the gas flow rate and pressure are not very high, so the separate solver is chosen with less memory.

In the choice of viscosity model, the gas film thickness used in the model is quite small, and the gas pressure is low, the gas flow rate is very slow, so the laminar flow model is chosen, which can both meet the required precision and the calculation is relatively low.

To the setting boundary conditions, they are only related to the pressure inlet, pressure outlet, and the fixed wall three boundary conditions. The boundary conditions of the 6 orifices are set at the pressure inlet boundary condition; in which the surface pressure and the absolute pressure, operating pressure have the following relations:

$$P_{absolute} = P_{gauge} + P_{operating} \tag{7}$$

In addition, the size of the surface pressure is the total pressure on the inlet boundary. For incompressible flow,

$$P_{total} = P_{static} + \frac{1}{2}\rho v^2 \tag{8}$$

For compressible flow,

$$P_{total} = P_{static}\left(1 + \frac{k-1}{2}Ma^2\right)^{k/(k-1)} \tag{9}$$

For the pressure outlet boundary conditions, the torus is selected as the pressure outlet boundary, shown in figure 4. In the CFD analysis software, the top and bottom two gas film surfaces (surface 3, surface 4) are set into a non-slip wall. It is needed to study the air bearing gas flow with faster diffusion, therefore do not consider the heat transfer effect of a fixed wall. From the above, the calculation of the air bearing of the actuator model can be derived.

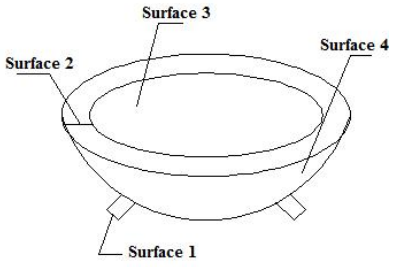

Fig.4. Diagrammatic sketch for setting boundary conditions

From the spherical air bearings in the standard model of the flow field pressure distribution shown in figure 5, it can be clearly seen that on the wall of the pressure distribution of the spherical air bearings is of symmetrical structure, so the equivalent pressure lines of the gas film are almost space concentric circles, beginning from the positions around the 6 orifices to the pressure outlet boundaries, the pressure value is constantly decreasing until decaying to zero at the pressure outlet locations. From the figure it can also be seen that the values in the 6 air feed orifices reach their maximum values and almost exactly the same.

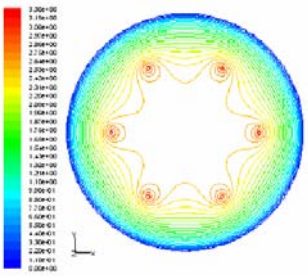

Fig.5. Pressure distribution of standard cases

In the case of changing the orifices' positions, the vortex torque effects by orifice 1 and the angle θ_1 between it and the vertical plane yo1z and the angle θ_2 between two orifices are investigated. In the standard model $\theta_1 = 30^\circ$, change θ_1 from 25 to 35 degrees and the pressure distribution diagram can be shown as figure 6. It can be seen from the diagram that when (a) = 25 degrees, the pressure around orifice 1 is larger than the other five orifices, caused the increase of bearing capacity; when θ_1 = 35 degrees, from the diagram (b) it can be seen that the pressure surrounding orifice 1 is relatively decreased and lower than the other five orifices' pressure, caused the bearing capacity decline.

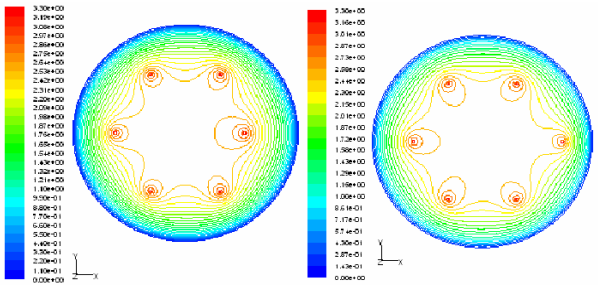

(a) (b)

Fig.6. Pressure distribution of different θ_1

(a) θ_1=25°, (b) θ_1=35°

Experimental results

Using the levitation and torque model, the closed-loop rotor position control can be realized based on the radial displacement to derive the stator current levitation component. The torque component can be adjusted by the ordinary PI controller. From the schematic illustration as shown in figure 7, the stator currents can be calculated and adopted to control 12 stator coils by the power electronics system. The drive unit for each coil is chosen as H bridge circuit respectively. The unit is integrated with IC and do not need to input detailed control signal for each switching device to control the magnitude and direction of currents with reducing the workload. The displacements PID,

rotation speed PI, torque and levitation force calculation are completed by DSP controller without additional analog circuit built.

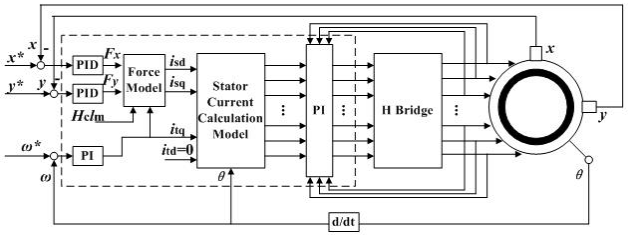

Fig.7. Illustration of control blocks of the electric drive

To validate the performance of the levitation system, experiments are carried out. Manufactured experiment prototype can be shown in figure 8. The length of output shaft is designed to 55mm and the angle resolution for three degree-of-freedom can averagely reach to 1 degree, which can meet the demands for most applications. The measured results of radial position of the rotor and the rotor speed change can be shown in figure 9. The spin rotation movement is in dynamic state and the displacements are measured by eddy currents sensor with relative 0.1 μ m accuracy. For the multi-DOF space motion measurement with respect to the initial position, the three Euler angles are able to be obtained from the CCD-based non-contact detection system with satisfied accuracy. From figure 9, it can be seen the rotor's position is limited in 150 μ m in levitation state with light load conditions. The errors have been controlled within satisfied range, with the presented control scheme.

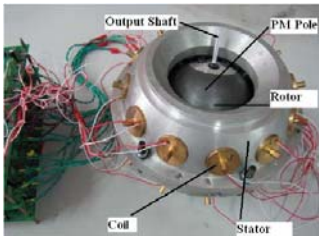

Fig.8. Experiment prototype of M-DOF actuator

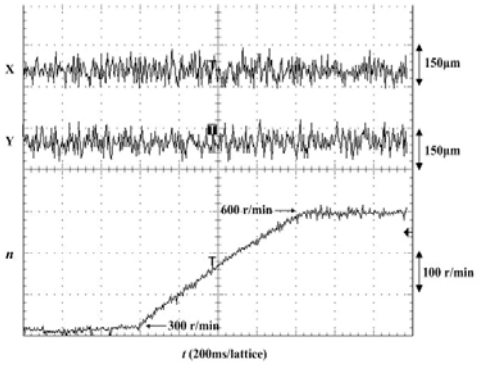

Fig.9. Measured waves of levitation process

Conclusions

This paper presents the modeling and spherical air bearing and levitation methodology for m-DOF actuator or motor applications. The method is applied in related industrial areas with its special features of advantages. In this work, the air bearing is used for basic supporting and pan-tilt motion with relatively large amplitude and fit for both spin rotation and slightly pan-tilt motions. Experiment is carried out to validate the effectiveness of presented methodology by setting a motion speed change in sequence. The results prove that the methodology is available and effective. It is expected that the presented scheme is able to provide a reference for further research and investigation for similar measurement problems of m-DOF actuators or motors.

Acknowledgements

This work was supported by the National Natural Science Foundation of China (under Grant No. 51107031, 50677013), the Natural Science Foundation of Hebei Province of China (under Grant No.E2009000703), the Foundation of Hebei Educational Committee (under Grant No.Z2010135), the Scientific Research Start Foundation of Doctoral Scholars of Hebei University of Science and Technology (under Grant No.QD200909) and the Funds for Distinguished Young Scholar of Hebei University of Science and Technology.

REFERENCES

[1] Kok-Meng Lee, Kun Bai and Jungyoul Lim, Dipole Models for Forward/Inverse Torque Computation of a Spherical Motor, *IEEE Transactions on Mechatronics*, 14 (2009) , No. 1, 46-54.

[2] Gregory S Chirikjian, David Stein, Kinematic design and commutation of a spherical stepper motor, *IEEE Trans. on Mechatronics*, 4 (1999) , No. 4, 342-353.

[3] W. Wang, J. Wang, G. W. Jewell and D. Howe, Design and Control of a Novel Spherical Permanent Magnet Actuator With Three Degrees of Freedom, *IEEE Transactions on Mechatronics*, 8 (2003) , No. 4, 457-468.

[4] Qunjing Wang, Zheng Li, Youyuan Ni, et al, Magnetic Field Computation of a PM Spherical Stepper Motor Using Integral Equation Method, *IEEE Trans. on Magnetics*, 42 (2006) , No. 4, 731-734.

[5] Byung-Il Kwon, Young-Boong Kim, Design and Analysis of Double Excited 3-Degree-of-Freedom Motor for Robots, *Journal of Electrical Engineering & Technology*, 6 (2011), No. 5, 618-625.

[6] Zheng Li, Analytical Calculation and Design of Permanent Magnets in a New Type Multi-DOF Motor Using Finite Element Method, *International Review of Electrical Engineering*, 6 (2011), No. 5, 2345-2350.

[7] Zheng Li, Yongtao Wang, Finite Element Analysis and Structural Optimization of a Permanent Magnet Spherical Actuator, *Electronics and Electrical Engineering*, 114 (2011), No. 8, 67-72.

[8] Zheng LI, Robust control of PM spherical stepper motor based on neural networks, *IEEE Transactions on Industrial Electronics*, 56 (2009) , No. 8, 2945-2954.

Authors: *Prof. Zheng LI is with the School of Electrical Engineering, Hebei University of Science and Technology, Yuhua East Road No.70, Shijiazhuang 050018, China. E-mail: Lzhfgd@163.com; He is the author of more than 60 published papers. His current research interests include design, analysis, and control of novel motors and actuators, intelligent control, and power electronics; Zhihu GUO, is currently working towards the MA.Eng. in the School of Electrical Engineering, Hebei University of Science and Technology. E-mail: guozhihu20@163.com.*